THE JOURNAL OF BIOLOGICAL CHEMISTRY VOL. 283, NO. 42, pp. 28297–28304, October 17, 2008

NMR Structure of the N-terminal Coiled Coil Domain of the Andes Hantavirus Nucleocapsid Protein*[S]

Received for publication, June 26, 2008, and in revised form, July 23, 2008 Published, JBC Papers in Press, August 7, 2008, DOI 10.1074/jbc.M804869200

Yu Wang[‡1], Daniel M. Boudreaux[§1], D. Fernando Estrada[‡], Chet W. Egan[‡], Stephen C. St. Jeor[§], and Roberto N. De Guzman[‡2]

From the [‡]Department of Molecular Biosciences, University of Kansas, Lawrence, Kansas 66045 and the [§]Department of Microbiology and Immunology, University of Nevada, Reno, Nevada 89557

The hantaviruses are emerging infectious viruses that in humans can cause a cardiopulmonary syndrome or a hemorrhagic fever with renal syndrome. The nucleocapsid (N) is the most abundant viral protein, and during viral assembly, the N protein forms trimers and packages the viral RNA genome. Here, we report the NMR structure of the N-terminal domain (residues 1–74, called N^{1-74}) of the Andes hantavirus N protein. N^{1-74} forms two long helices (α_1 and α_2) that intertwine into a coiled coil domain. The conserved hydrophobic residues at the helix α_1-α_2 interface stabilize the coiled coil; however, there are many conserved surface residues whose function is not known. Site-directed mutagenesis, CD spectroscopy, and immunocytochemistry reveal that a point mutation in the conserved basic surface formed by Arg^{22} or Lys^{26} lead to antibody recognition based on the subcellular localization of the N protein. Thus, Arg^{22} and Lys^{26} are likely involved in a conformational change or molecular recognition when the N protein is trafficked from the cytoplasm to the Golgi, the site of viral assembly and maturation.

Hantaviruses can cause two emerging infectious diseases known as the hantavirus cardiopulmonary syndrome (HCPS)[3] and the hantavirus hemorrhagic fever with renal syndrome (1). Annually, there are over 150,000 cases of hantaviral infections reported world wide (2). Rodents are the primary reservoir of hantaviruses, and humans are normally infected by inhalation of aerosol contaminated with the excreta of infected rodents. The first reported cases of HCPS in North America (3) was caused by a novel hantaviral species (4, 5), the Sin Nombre virus, and had an initial mortality rate of 78%. HCPS has since been reported throughout the United States with a current mortality rate of 35% when correctly diagnosed (6). The major cause of HCPS in South America is the Andes virus, and person-to-person transmission of the Andes virus was reported in Argentina and Chile (7). Hantaviruses are known to invade and replicate primarily in endothelial cells, including the endothelium of vascular tissues lining the heart (8–10).

The genome of hantaviruses consists of three negative-stranded RNAs, which encode the nucleocapsid (N) protein, two integral membrane glycoproteins (G1 and G2), and an RNA-dependent RNA polymerase (L protein). The N protein is highly immunogenic (11, 12) and elicits a strong immune response, which confers protection in mice (13–15). It is highly conserved and is the most abundant viral protein, and it plays important roles in viral encapsidation, RNA packaging, and host-pathogen interaction (16). The N protein binds to viral proteins (16), host proteins (17–23), and viral RNA (24–28). The self-association of the N protein into trimers was shown by gradient fractionation and chemical cross-linking (29). Deletion mapping identified that regions at the N and C termini are important in N-N interaction (29–31), and a model of trimerization was proposed based on the head-to-head and tail-to-tail association of the N-terminal and C-terminal domains, respectively (30, 32).

The N-terminal region in the Sin Nombre virus N protein (residues 3–73) (33) and the Tula virus (residues 1–77) (34) were predicted to form coiled coil domains. Recently, the structure of the N-terminal coiled coil domain (residues 1–75 and 1–93) of the Sin Nombre virus was determined by crystallography (35). The highly conserved hydrophobic residues stabilize the structure of the coiled coil; however, there are highly conserved polar residues that appear to have no function in stabilizing the coiled coil domain. Here, we report the solution structure of the N-terminal 1–74 residues of the Andes virus N protein, which also forms a coiled coil domain. Further, we identified that the coiled coil contains distinct regions of positively and negatively charged surfaces involving conserved polar residues. We hypothesize that these regions are also important in N protein function. We used site-directed mutagenesis to alter the surface of the N protein and assayed for the subcellular localization of the N protein by immunocytochemistry. We used CD spectroscopy to confirm that mutations did not alter the coiled coil structure of the N^{1-74} (residues 1–74 of the N protein) domain. However, immunocytochemistry showed that despite the N protein being present throughout the cytoplasm, a monoclonal antibody

* This work was supported, in whole or in part, by National Institutes of Health Grants AI057160 and AI65359. This work was also supported by American Heart Association Grant 0755724Z (to R. N. D.); National Science Foundation Program Grant EF 0326999 (to S. C. S. J.). The costs of publication of this article were defrayed in part by the payment of page charges. This article must therefore be hereby marked "*advertisement*" in accordance with 18 U.S.C. Section 1734 solely to indicate this fact.

[S] The on-line version of this article (available at http://www.jbc.org) contains supplemental Figs. S1–S3.

[1] These authors contributed equally to this work.

[2] To whom correspondence should be addressed: Dept. of Molecular Biosciences, University of Kansas, 1200 Sunnyside Ave., Lawrence, KS 66045. Fax: 785-864-5294; E-mail: rdguzman@ku.edu.

[3] The abbreviations used are: HCPS, hantavirus cardiopulmonary syndrome; HSQC, heteronuclear single quantum coherence; HMQC, heteronuclear multiple quantum coherence; N, nucleocapsid protein; NOE, nuclear Overhauser effect; NOESY, NOE spectroscopy.

only recognized the Arg^{22} and Lys^{26} mutants when nucleocapsids are associated with the Golgi, the site of viral assembly and maturation. We propose that the conserved surface residues Arg^{22} and Lys^{26} are important in the proper conformation or molecular recognition of the N protein.

EXPERIMENTAL PROCEDURES

Protein Expression and Purification of N^{1-74}—The N^{1-74} domain of the Andes virus (strain 23) nucleocapsid protein was subcloned into pET151 (Invitrogen), which appends a 33-residue His_6 tag and a TEV (tobacco etch virus) protease cleavage site at the N terminus. Isotopically (^{15}N,^{13}C) labeled protein was overexpressed in *Escherichia coli* BL21(DE3) (DNAY) grown in 1 liter of M9 minimal medium with [^{15}N]ammonium chloride and [^{13}C]glucose. The cells were grown at 37 °C to A_{600} 0.8, induced with 1 mM isopropyl-β-D-thiogalactopyranoside, and incubated overnight (16 h) in a 15 °C shaker. The cells were harvested by centrifugation, resuspended in 30 ml of binding buffer (20 mM Tris-HCl, pH 8.0, 500 mM NaCl, 5 mM imidazole), and lysed by sonication. The cells were centrifuged at 22,500 × *g* for 15 min, and the supernatant was loaded on a Ni^{2+} affinity column (Sigma), washed with 35 ml of binding buffer, and eluted with elution buffer (500 mM NaCl, 20 mM Tris-HCl, pH 8.0, 250 mM imidazole). The purified His-tagged N^{1-74} was dialyzed into buffer (10 mM sodium phosphate, pH 6.9, 10 mM NaCl) and used for NMR structure determination. Typical NMR samples contained 1–1.4 mM N^{1-74}. For CD spectroscopy, the His tag was cleaved by adding 0.08 mM TEV protease into purified His-tagged N^{1-74} and dialyzing the mixture in an 8000 molecular mass cut-off dialysis tubing in buffer (50 mM Tris-HCl, pH 8.0, 0.5 mM EDTA, 1 mM dithiothreitol) for 16 h at room temperature.

Mutagenesis of N^{1-74}—Site-specific mutations in the N^{1-74} domain were introduced by PCR using the Stratagene QuikChange kit in two plasmids: (i) pET151-N^{1-74}, used to overexpress recombinant His-tagged N^{1-74} in *E. coli*, and (ii) pcDNA3.1-AND-N, used to express full-length Andes virus N protein in a mammalian cell line for immunocytochemistry (see below). The mutations were confirmed by DNA sequencing.

NMR Spectroscopy—NMR data were acquired at 25 °C using a Bruker Avance 800 MHz spectrometer equipped with a cryoprobe, processed with NMRPipe (36), and analyzed with NMRView (37). Backbone assignments were obtained from two-dimensional ^{1}H-^{15}N HSQC (38) and three-dimensional HNCA (39), CBCA(CO)NH (39), HNCACB (40), and HNCO (41). Secondary structures were identified from the C^{α}, C^{β}, C', and H^{α} chemical shifts (42). Side chain assignments were obtained from two-dimensional ^{1}H-^{13}C HMQC (43), three-dimensional HBHA(CO)NH (44), and three-dimensional ^{13}C-edited HMQC-NOESY (t_{mix} = 120 ms) (45). Nuclear Overhauser effect (NOE) cross-peaks were identified from three-dimensional ^{15}N-edited NOESY-HSQC (t_{mix} = 120 ms) (46) and three-dimensional ^{13}C-edited HMQC-NOESY (t_{mix} = 120 ms) (45). Hydrogen-deuterium exchange was performed by lyophilizing a 600-μl ^{15}N-labeled NMR sample and resuspending in 600 μl of 50% D_2O, 50% H_2O, followed by acquisition of six consecutive 20-min two-dimensional ^{1}H-^{15}N HSQC spectra. Peak volumes were analyzed to identify residues with slower hydrogen-deuterium exchange rates.

Structure Calculation—NOE distance restraints were classified into upper bounds of 2.7, 3.5, 4.5, and 5.5 Å and lower bound of 1.8 Å based on peak volumes. Backbone dihedral angles in the α-helical regions were restrained to φ ($-60 \pm 20°$) and ψ ($-40 \pm 20°$). Hydrogen bonding distance restraints were used for α-helical residues that showed slow hydrogen-deuterium exchange rates. Initial structures were generated by torsion angle dynamics in CYANA (47), followed by molecular dynamics and simulated annealing in AMBER7 (48), first *in vacuo* and then with the generalized Born potential to account for the effect of solvent during structure calculation. CYANA and AMBER structure calculation protocols have been described elsewhere (49). Iterative cycles of AMBER calculations followed by refinement of NMR-derived restraints were performed until the structures converged with low restraint violations and good statistics in the Ramachandran plot. A family of 20 lowest energy structures was analyzed using PROCHECK (50), and graphics were generated using Pymol. The surface electrostatic potentials were calculated using APBS (51) and visualized in Pymol.

CD Spectroscopy—N^{1-74} samples for CD spectroscopy contained 5–10 μM protein in buffer (25 μM Tris-HCl, pH 8, 3 μM EDTA, and 5 μM dithiothreitol). CD spectra were collected on a Jasco J-815 spectropolarimeter in triplicate. Wavelength scans were collected at 25 °C at a scanning rate of 50 nm/min. Thermal denaturation scans at 222 nm were acquired with a temperature ramp rate of 1 °C/min to a final temperature of 80 °C, followed by cooling at 1 °C/min to 25 °C. The melting temperature (T_m) was determined from calculating the first derivative of thermal denaturation plots using the Jasco CD software.

Immunocytochemistry—Immunocytochemistry was performed as reported (52). Briefly, Cos-7 cells (ATCC; no. CRL-1651) were grown overnight in 24-well plates with coverslips at 37 °C and 5% CO_2 in Dulbecco's modified Eagle's medium containing 10% fetal bovine serum. The cells at 80% confluence were transfected using Lipofectamine 2000 (Invitrogen) with 0.8 μg of pcDNA3.1-AND-N plasmid, which expresses full-length wild type or mutated N protein. At 48 h after transfection, the cells were washed with ice-cold phosphate-buffered saline and fixed at room temperature with methanol:acetone (3:1) for 10 min. The cells were incubated in 10 mM glycine for 30 min and permeabilized in phosphate-buffered saline with 0.1% Triton X-100 for 30 min. Permeabilized cells were incubated with antibodies for 60 min at room temperature and washed for 5 min three times with 0.3% Tween in phosphate-buffered saline after each incubation. Goat serum (10%) was used as a blocking agent. Primary antibodies were of two sets: (i) rabbit polyclonal anti-hantavirus nucleocapsid (1:1000) (Immunology Consultants Laboratory; no. RSNV-55) and mouse monoclonal anti-hantavirus-nucleocapsid (1:1000) (Abcam; no. AB34757) or (ii) rabbit anti-Golgi matrix protein GM130 (1:200) (Calbiochem; no. CB1008) and mouse-anti-hantavirus nucleocapsid (1:1000). Secondary antibodies used were Alexa-Fluor-488 (1:1000) (Invitrogen; no. A11008) and Alexa-Fluor-594 (1:1000) (Invitrogen; no. A11005). Lastly, the cells were stained with 4′,6-diamidino-2-phenylindole (Bio-

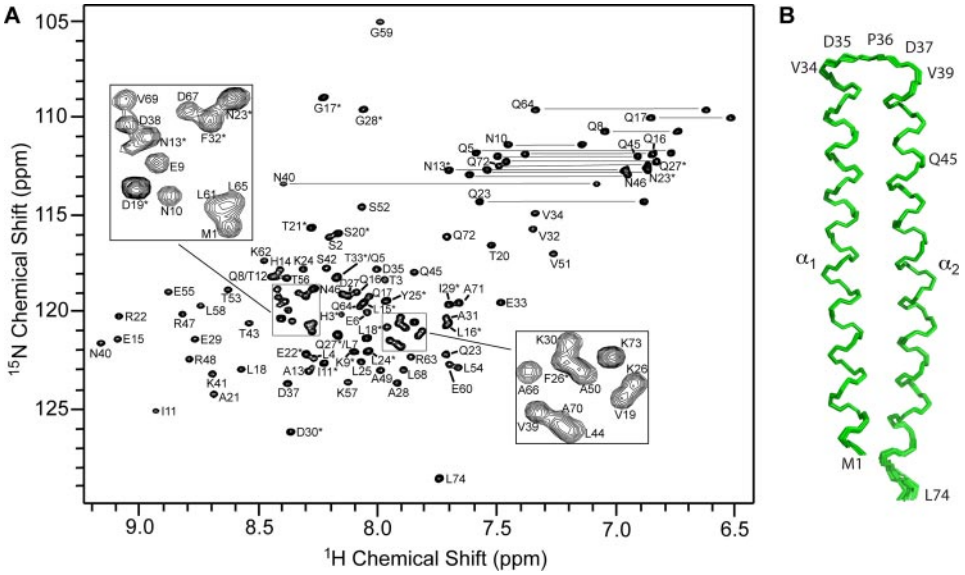

FIGURE 1. *A*, assigned ^{1}H-^{15}N HSQC spectrum of Andes virus N^{1-74} domain. The 33 N-terminal residues (shown with *asterisks*) are part of the His tag introduced by pET151. The *boxes* show expansions of the crowded regions. *B*, superposition of 20 low energy NMR structures of the Andes virus N^{1-74} coiled coil domain. N^{1-74} forms two α-helices, Met^{1}–Val^{34} and Val^{39}–Leu^{74}. The anti-nucleocapsid monoclonal antibody used in immunocytochemistry below recognizes an epitope somewhere between residues 1 and 45.

Genex; no. CS2010-06), mounted on slides, and visualized at 60× on an Olympus FV1000 confocal microscope. The images were cropped and adjusted using Adobe Photoshop CS2.

RESULTS

NMR Structure Determination of N^{1-74}—The His-tagged N^{1-74} expressed well in soluble form in *E. coli* and yielded an excellent two-dimensional ^{1}H-^{15}N HSQC spectrum that showed distinct and well dispersed peaks (Fig. 1*A*). Nearly complete backbone assignments were obtained from three-dimensional HNCA, CBCA(CO)NH, HNCACB, and ^{15}N-edited NOESY-HSQC. The histidine residues of the His tag were overlapped and could not be assigned unambiguously. The C^{α}, H^{α}, C^{β}, and C' secondary chemical shifts (supplemental Fig. S2) showed that the first 33 residues, which were part of the His tag, were in random coil orientation, and the native N^{1-74} sequence contained two α-helices (42). Side chain assignments were completed using two-dimensional ^{1}H-^{13}C HMQC, three-dimensional HBHA(CO)NH, and three-dimensional ^{13}C-edited HMQC-NOESY. Manual analysis of three-dimensional ^{15}N- and ^{13}C-edited NOESY spectra identified 1432 unambiguous interproton distance restraints. The NOE restraints together with 73 φ and 62 ψ dihedral angle restraints and 38 hydrogen bond restraints (supplemental Table S1) were used in structure calculation and refinement in CYANA and AMBER. The 20 low energy NMR structures of N^{1-74} converged into a family of structures (Fig. 1*B*) with low restraint violations and good Ramachandran plot statistics (supplemental Table S1).

The N^{1-74} Coiled Coil Domain—N^{1-74} forms two well defined α-helices (α_1, Met^{1}–Val^{34}; α_2, Val^{39}–Leu^{74}) that are connected by an ordered acidic loop (Asp^{35}-Pro^{36}-Asp^{37}-Asp^{38}) (Fig. 1*B*). The two helices are intertwined into a coiled coil, and the helix α_1-α_2 interface is lined with hydrophobic amino acids positioned in every seventh residue on helix α_1 (Leu^{4}, Ile^{11}, Leu^{18}, Leu^{25}, and Val^{32}) and helix α_2 (Leu^{44}, Val^{51}, Leu^{58}, and Leu^{65}) (Fig. 2*A*). This heptad repeat of hydrophobic residues is a hallmark of coiled coils and is highly conserved among hantaviruses (34). Together with Pro^{36}, the heptad repeats of leucines, isoleucines, and valines form the hydrophobic core that stabilize the structure of the coiled coil (Fig. 3*A*). On the same face of the hydrophobic heptad, there is another seven-residue repeat, in this case, composed of polar residues on helix α_1 (Gln^{8}, Glu^{15}, Arg^{22}, and Glu^{29}) (Fig. 2*B*), which are invariant among the hantaviruses (supplemental Fig. S1). Helix α_2 also contains a polar heptad, however, with more residue variability at positions 41 (Lys), 48 (Arg/Gln/Glu), 55 (Glu/Gln), and 62 (Lys/Arg). These polar residues form two conserved salt bridges between helix α_1-α_2 (Glu^{15}–Lys^{62} and Arg^{22}–Glu^{55}) (Fig. 2*B*). Gln^{8} and Lys^{41} are surface-exposed and do not form any salt bridges; however, they are invariant among the hantaviruses, suggesting some unknown function.

In addition to the conserved heptad repeats mentioned above, there are other highly conserved residues whose side chains are pointed toward the helix α_1-α_2 interface. These residues are nonpolar (Leu^{7} and Leu^{54}), aromatic (His^{14}), polar (Gln^{17}, Asn^{40}, and Thr^{43}), or charged (Glu^{6}, Glu^{15}, Glu^{29}, Lys^{41}, Arg^{47}, and Lys^{57}), and their side chains are pointed toward the helix α_1-α_2 interface (Fig. 2*C*). The polar and charged residues in this group do not participate in any salt bridge or hydrogen bonding contacts; however, their polar moieties are pointed toward the surface of the coiled coil, whereas the aliphatic portion of their side chains are involved in hydrophobic interaction that contribute to the stabilization of the hydrophobic core. The methyl groups of two invariant alanines, Ala^{21} and Ala^{28}, in helix α_1 (Fig. 2*C*) are oriented toward the helix α_1-α_2 interface but do not contact any other residues on helix α_2, indicating that small side chains are required in those positions.

Conserved Surface Residues—A striking feature of the N^{1-74} coiled coil is the presence of large numbers of highly conserved residues whose side chains are pointed away from the coiled coil. These residues are nonpolar (Ala^{66} and Val^{19}), polar (Gln^{8} and Gln^{23}), basic (Lys^{24}, Lys^{26}, Arg^{63}, and Lys^{73}), and acidic (Asp^{27}, Glu^{33}, Asp^{35}, Asp^{37}, Asp^{38}, Glu^{60}, and Asp^{67}) (Fig. 2, *B* and *C*). These polar residues are identical (Gln^{8}, Gln^{23}, Lys^{24}, Glu^{33}, Asp^{35}, Asp^{37}, Arg^{63}, and Lys^{73}) or semi-identical (basic residues in position 26 and acidic residues in positions 27, 38, and 60) among hantaviruses (supplemental Fig. S1). Further, many residues in this group are clustered together on the surface. The first cluster (Gln^{23}, Lys^{24}, and Lys^{26} together with Arg^{47} and Arg^{22} discussed in the preceding paragraph) forms a basic surface (Fig. 2*D*), and the second cluster (Asp^{27}, Glu^{33},

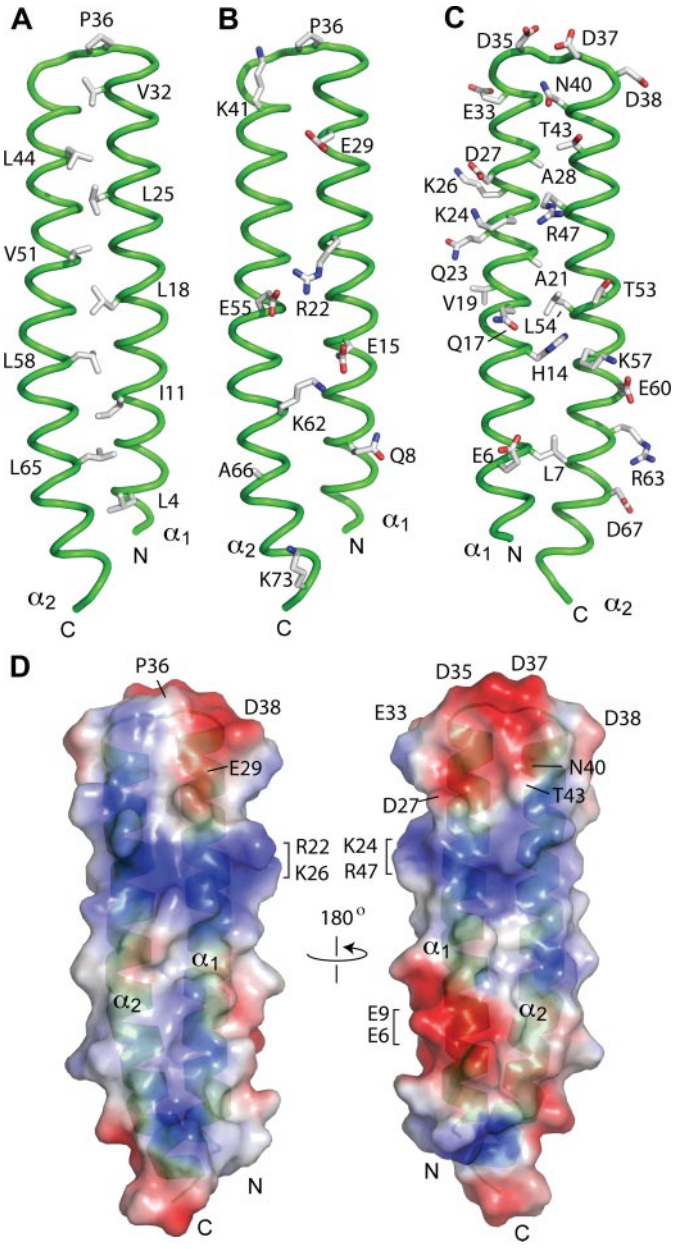

FIGURE 2. *A*, heptad repeats of conserved hydrophobic residues form the interface of the helix α_1 and α_2 that stabilize the coiled coil domain. *B*, there is also a heptad repeat of polar residues, some of which (Arg^{22}–Glu^{55} and Glu^{15}–Lys^{62}) form salt bridges that contribute in stabilizing the coiled coil. *C*, there are many highly conserved residues that point away from the coiled coil and thus are not involved in stabilizing the coiled coil. *D*, electrostatic surface potential map of N^{1-74}. The orientation of the *left panel* is identical to that in *A* and is rotated 180° from the *right panel*, which is identical in the orientation of *C*. Conserved surface residues forming the acidic (*red*) and basic (*blue*) surfaces are indicated. Point mutations of Arg^{22} and Lys^{26} had a dramatic effect on the antibody recognition of the N protein *in vivo*.

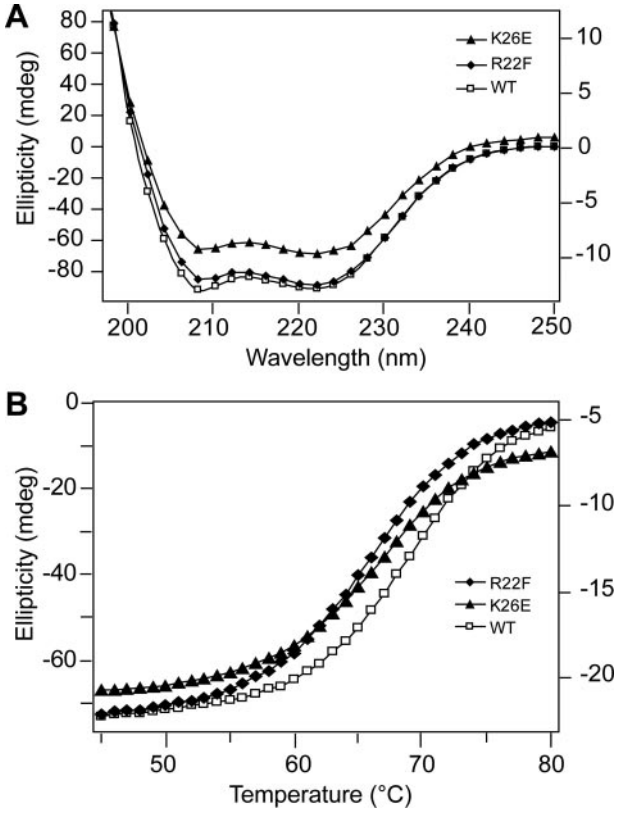

FIGURE 3. *A*, CD spectra of N^{1-74} wild type (*WT*) and point mutants (K26E and R22F) showing the characteristic α-helical dips at 208 and 222 nm. All other N^{1-74} point mutants (listed in Table 1) showed similar α-helical CD spectra. *B*, CD thermal denaturation curves, monitored at 222 nm, of wild type N^{1-74} and two point mutants, K26E and R22F. The rest of the point mutants showed similar thermal denaturation curves. The ellipticity scales on the *y* axes are shown on *left* (wild type and R22F) and *right* (K26E).

Asp^{35}, Asp^{37}, and Asp^{38}) forms an acidic surface (Fig. 2*D*). We mutagenized many residues in this group (see below) to test the hypothesis that these residues are important in molecular recognition rather than in stabilizing the coiled coil structure.

Electrostatic Surface of N^{1-74}—The N^{1-74} domain is acidic (theoretical pI of 5.8), and the surface electrostatic potential map of N^{1-74} shows distinct regions of negatively charged (*red*) and positively charged (*blue*) surfaces (Fig. 2*D*). The tip of the coiled coil, where the loop connecting the two helices are located, is negatively charged (Fig. 2*D*) because of clustering of conserved acidic residues (Asp^{27}, Glu^{29}, Glu^{33}, Asp^{35}, Asp^{37}, and Asp^{38}) and polar residues (Asn^{40} and Thr^{43}). Although the N^{1-74} domain is acidic, there are conserved basic residues (Arg^{22}, Lys^{24}, Lys^{26} and Arg^{47}) that form a positively charged surface just below the negatively charged tip (Fig. 2*D*). Point mutations in this positively charged surface have a dramatic effect on the antibody recognition of the N protein *in vivo* (see below).

In addition, there is a smaller negatively charged surface formed by Glu^{9} and Glu^{6} (Fig. 2*D*). Residue 9 could be acidic (Glu or Asp) or basic (Arg or Lys). Residue 9 is acidic among American hantaviruses (which cause the cardiopulmonary syndrome) and Old World hantaviruses that are nonpathogenic or cause a milder form of hemorrhagic fever with renal syndrome. Residue 9 is basic among Old World hantaviruses that causes the severe form of hemorrhagic fever with renal syndrome.

Circular Dichroism Spectroscopy of N^{1-74}—Point mutations were introduced in the basic (Arg^{22}, Lys^{24}, Lys^{26}, and Arg^{47}) and acidic (Glu^{33} and Asp^{38}) surfaces. In addition, we mutated Gln^{23}, which is near the basic region, and Pro^{36}, which is near the acidic region. These residues are surface-exposed (Fig. 2*D*) and are nearly invariant among hantaviruses (supplemental Fig. S1). CD spectroscopy was used to assess the folding and stability of N^{1-74} mutants. Wild type and point mutants showed

TABLE 1
Melting temperatures (T_m) and ellipticity (θ) ratio at 222 and 208 nm of N^{1-74}

N^{1-74}	T_m	$\theta_{222}/\theta_{208}$	Change in surface property
	°C		
D38R	64.3 ± 0.01	1.06	Acidic to basic
E33K	64.4 ± 0.02	1.05	Acidic to basic
P36G	66.0 ± 0.1	0.99	Increased loop flexibility
R47E	66.0 ± 0.03	1.07	Basic to acidic
D38L	66.2 ± 0.01	1.03	Acidic to nonpolar
R22F	66.4 ± 0.1	1.07	Basic to bulky nonpolar
K26E	67.0 ± 0.02	1.04	Basic to acidic
E33L	67.4 ± 0.01	1.07	Acidic to nonpolar
Q23L	68.5 ± 0.03	1.01	Polar to nonpolar
R22M	69.3 ± 1.2	1.06	Basic to nonpolar
WT	69.4 ± 0.1	0.99	No change
K24A	70.6 ± 0.01	1.04	Basic to small nonpolar
R47A	74.0 ± 0.02	1.02	Basic to small nonpolar

nearly identical CD spectra (Fig. 3*A*), indicating that the α-helical structure of N^{1-74} was preserved. In addition, the ratio of ellipticity at 222 and 208 nm can be used to characterize α-helices. A $\theta_{222}/\theta_{208}$ ratio of ~1.0 indicates α-helices with extensive interhelical contacts as in coiled coils and helical bundles, whereas a $\theta_{222}/\theta_{208}$ ratio of ~0.8 indicates extended α-helices with little interhelical contacts (53–55). All N^{1-74} constructs have a $\theta_{222}/\theta_{208}$ ratio higher than 0.9 (Table 1), suggesting that all mutants have the intact coiled coil structure. Further insight was provided by acquiring the CD melting temperatures (Fig. 3*B* and Table 1). Compared with wild type N^{1-74}, the majority of mutants showed lower T_m, with D38R having the lowest value, whereas two mutants (K24A and R47A) showed higher T_m (Table 1). Nevertheless, all mutations were within ±5 °C of wild type T_m (Table 1), indicating that the mutations did not drastically alter the thermal stability of N^{1-74}. Thus, the point mutations maintained the structural integrity of the N^{1-74} coiled coil.

Immunocytochemistry of N Protein—Hantaviruses are believed to mature intracellularly; specifically, in the Golgi complex (56). During infection, the N protein was shown to localize cytoplasmically in the endoplasmic reticulum-Golgi intermediate compartment, presumably as they traffic from the endoplasmic reticulum to the Golgi (22). In addition, immunofluorescence of Cos-7 cells transfected with the N protein alone showed a granular pattern of staining in the perinuclear region (32, 34), suggesting colocalization with the Golgi. To test our hypothesis that the conserved surface residues of N^{1-74} are important in molecular interaction, we introduced point mutations designed to keep the N^{1-74} coiled coil domain intact while altering only specific surface residues and transfected full-length N protein in mammalian cells to observe the subcellular localization of the N protein. We used two types of anti-nucleocapsid antibodies, rabbit polyclonal and mouse monoclonal antibodies. The polyclonal antibody detected that wild type N and mutants (Arg^{22}, Gln^{23}, Lys^{24}, and Lys^{26}) were located throughout the cytoplasm (Fig. 4*A*). The monoclonal antibody also detected wild type N and the Gln^{23} and Lys^{24} mutants throughout the cytoplasm in a similar pattern of staining as the polyclonal antibody (Fig. 4*A*). However, the monoclonal antibody showed a dramatic difference between the recognition of wild type N and the Arg^{22} and Lys^{26} mutants (Fig. 4*A*). Using the monoclonal antibody, Arg^{22} and Lys^{26} mutants were observed in a compact location lateral to the nucleus (Fig. 4*A*). To further define the subcellular localization of these N mutants, a Golgi-specific antibody (targeting the Golgi matrix protein GM130) was used (Fig. 4*B*). The Arg^{22} and Lys^{26} mutants were only detected by the monoclonal antibody when the N protein colocalized with the Golgi (Fig. 4*B*); however, these mutants were also present throughout the cytoplasm as shown by the polyclonal antibody (Fig. 4*A*). Thus, for the Arg^{22} and Lys^{26} mutants, the monoclonal antibody was able to distinguish between two populations of the N protein based on its subcellular localization in the cytoplasm or in the Golgi, the site of viral assembly and maturation (56). Other mutants (Glu^{33}, Asp^{35}, Pro^{36}, Asp^{37}, Asp^{38}, and Arg^{47}) did not show this localization-dependent antibody recognition (supplemental Fig. S3).

DISCUSSION

The NMR structure of the Andes virus N^{1-74} domain is similar to the recent crystal structure of the Sin Nombre virus nucleocapsid protein N-terminal coiled coil (N^{1-75}) (35). The Cα root mean square deviation between the two structures is 1.3 Å. The crystal structure determination of the N protein addressed the issue of the trimerization of the N protein (35) because earlier models suggested the trimerization of the nucleocapsid N-terminal domain (29, 30, 32, 33). A proposed model of N protein trimerization involves, first, the association of three N-terminal domains, followed by the association of three C-terminal domain (34). However, crystallography revealed that the Sin Nombre nucleocapsid N-terminal domain was monomeric and formed a coiled coil structure, and conserved hydrophobic residues participate in helix-helix interaction that stabilize the coiled coil (35). Our NMR structure of the Andes virus N^{1-74} supports the crystallographic results; even at 1.4 mM, N^{1-74} remained monomeric in solution. Our results, however, do not preclude the trimerization of full-length N protein *in vivo* by another mechanism.

A feature of the N^{1-74} domain that had not been addressed in the literature is the role of many conserved polar residues whose side chains are pointed away from the coiled coil. Furthermore, the majority of these surface-exposed residues are not involved in polar interactions (Fig. 2*D*). Point mutations of these polar residues maintained the structural integrity and high thermal stability of the coiled coil (Fig. 3 and Table 1). For example, Arg^{22}, which forms a salt bridge with a conserved residue Glu^{55}, can be mutated (R22F or R22M) without disrupting the coiled coil structure of N^{1-74} (Table 1). R22F, which replaced arginine with a bulkier aromatic side chain, decreased the overall melting temperature by ~3 °C (Table 1). This change is likely attributed to increased steric clash between phenylalanine and Glu^{55}. However, the observation that R22M melts at a temperature comparable with that of wild type suggests that the salt bridge between Arg^{22} and Glu^{55} does not play a significant role in helix-helix interaction and that hydrophobic interaction is the major force stabilizing the coiled coil. A mutation in a nonpolar residue, Pro^{36}, which is at the turn connecting the two α-helices of the coiled coil, had a T_m approximately four degrees lower than wild type, which is consistent

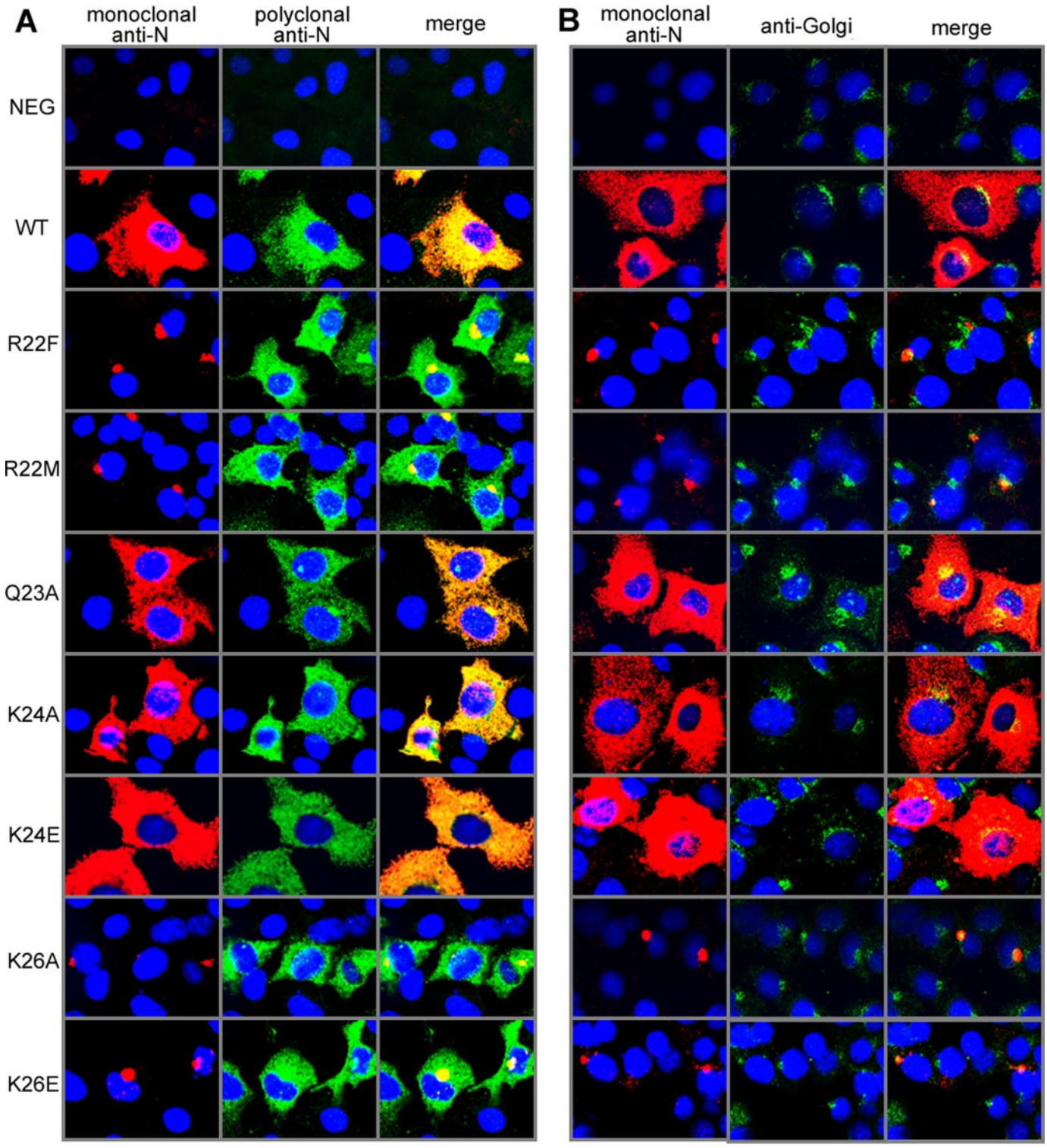

FIGURE 4. **Immunocytochemistry of full-length N protein with point mutations in the N^{1-74} coiled coil domain.** Cos-7 cells were transfected with a plasmid expressing Andes virus N protein. Two days after transfection, the cells were fixed for immunofluorescence microscopy and double labeled with monoclonal (*red*) and polyclonal (*green*) anti-nucleocapsid antibodies (*A*) and monoclonal anti-nucleocapsid antibody (*red*) and anti-Golgi antibody (*green*) (*B*). The cell nuclei were stained *blue* using 4′,6-diamidino-2-phenylindole. Point mutations in Arg^{22} and Lys^{26} showed a dramatic difference in the monoclonal antibody recognition of Golgi-associated N protein, suggesting that the conformation or molecular interaction (or both) of the N protein is different when it is in the cytoplasm or when it is associated with the Golgi. *WT*, wild type.

with a mutation that increases the number of conformations available at the Pro^{36} turn and destabilizes the overall protein structure by uncoupling the helix-helix interaction. Nevertheless, all of the point mutations of the conserved surface residues maintained the coiled coil structure of N^{1-74} (Fig. 3 and Table 1).

Thus, there is no compelling structural reason for the high sequence conservation of surface residues. Furthermore, these

polar residues are clustered together on the surface of the N^{1-74} domain and form distinct positively and negatively charged regions (Fig. 2*D*). We hypothesize that the reason for the clustering of conserved polar residues on the surface of N^{1-74} is that they are sites of molecular recognition involved in the proper function of the N protein. Our mutagenesis and immunocytochemistry data suggest that point mutations in this group had a dramatic effect on the antibody recognition of the N protein with respect to its subcellular localization (Fig. 4).

During infection, nucleocapsids are trafficked to the cytoplasm (22) to assemble into mature virions (56). Mammalian cells transfected with the N protein alone show a granular pattern of immunofluorescence (32, 34). This localization pattern is thought to be necessary for the nucleocapsid to perform its many functions in the establishment of an effective infection (22). We questioned whether the conserved polar surface residues in the coiled coil domain are important in the proper functioning of the N protein and reasoned that defects in the conformation or molecular recognition of the N protein will be manifested in the antibody recognition of the N protein in the context of its subcellular localization. CD spectroscopy confirmed that the mutant forms of N^{1-74} maintained the structural integrity of the coiled coil structure (Fig. 3 and Table 1); thus, the mutations altered only the surface property of the N protein.

Immunocytochemistry (Fig. 4) indicates that mutations in a conserved basic surface formed by Arg^{22} and Lys^{26} show monoclonal antibody recognition depending on the subcellular localization of the N protein. Polyclonal antibodies show that Arg^{22} and Lys^{26} mutants are present in the cytoplasm and Golgi; however, only Golgi-associated mutant nucleocapsids are detected by the monoclonal antibody (Fig. 4). Mutation of Arg^{22} or Lys^{26} changes the presentation of the N-terminal coiled coil to the monoclonal antibody. This change is dependent on the subcellular localization of the N protein.

There are two possible scenarios that could account for this differential monoclonal antibody recognition of the Arg^{22} and Lys^{26} mutants. First, there may be a difference in the conformation of the N-terminal coiled coil depending on whether the N protein is localized in the cytoplasm or in the Golgi, and this conformational change upon binding to the Golgi exposes the epitope, which is somewhere between residues 1–45 (comprising helix α_1, the interhelical loop, and part of helix α_2 of the N^{1-74} coiled coil; Fig. 1*B*), thereby allowing the monoclonal antibody to recognize the N protein associated with the Golgi. Second, the epitope may be masked differently by molecular interactions when the N protein is localized in the cytoplasm or in the Golgi. In addition to self-association, several host proteins such as SUMO-1 (17–19), Ubc9 (17, 18), Daxx (20), actin (21), microtubules (22), and MxA (23) were reported to bind the N protein. Binding of the N protein with SUMO-1 and Ubc9 was required for localization of the N protein in the perinuclear region (17, 19). Furthermore, because the N protein is not known to be a membrane protein, its localization in the Golgi must involve interaction with a Golgi-associated protein. Any of these molecular interactions could potentially alter the epitope presentation of the N^{1-74} coiled coil and needs to be experimentally verified.

In summary, our structural results revealed that the highly conserved polar residues in the N-terminal coiled coil domain of the hantavirus nucleocapsid protein form distinct acidic and basic surfaces, and point mutations of the conserved basic surface formed by Arg^{22} and Lys^{26} allowed a monoclonal antibody to distinguish between two populations of the N protein based on its subcellular localization. Thus, in the Arg^{22} or Lys^{26} mutants, the conformation or molecular interaction of the N protein is different when it is in the cytoplasm or in the Golgi, the site of viral assembly and maturation.

Acknowledgments—We are grateful to Albert Rizvanov (University of Nevada, Reno) for constructing the N^{1-74} expression plasmid, Evan Colletti (University of Nevada, Reno) and Mariana Bego (University of Nevada, Reno) for guidance in confocal microscopy, and Thenmalarchelvi Rathinavelan (University of Kansas), Gaya Amarasinghe (Iowa State University), and Edina Harsay (University of Kansas) for critical reading of the manuscript.

REFERENCES

1. Schmaljohn, C., and Hjelle, B. (1997) *Emerg. Infect. Dis.* **3,** 95–104
2. Khaiboullina, S. F., Morzunov, S. P., and St. Jeor, S. C. (2005) *Curr. Mol. Med.* **5,** 773–790
3. Koster, F., Levy, H., Mertz, G., Young, S., Foucar, K., McLaughlin, J., Bryt, B., Merlin, T., Zumwalt, R., McFeely, P., Nolte, K., Burkhart, M., Kalishman, N., Gallaher, M., Voorhees, R., *et al.* Centers for Disease Control and Prevention (1993) *Morbid. Mortal. Weekly Rep.* **42** 421–424
4. Nichol, S. T., Spiropoulou, C. F., Morzunov, S., Rollin, P. E., Ksiazek, T. G., Feldmann, H., Sanchez, A., Childs, J., Zaki, S., and Peters, C. J. (1993) *Science* **262,** 914–917
5. Hjelle, B., Jenison, S., Torrez-Martinez, N., Yamada, T., Nolte, K., Zumwalt, R., MacInnes, K., and Myers, G. (1994) *J. Virol.* **68,** 592–596
6. Mertz, G. J., Hjelle, B., Crowley, M., Iwamoto, G., Tomicic, V., and Vial, P. A. (2006) *Curr. Opin. Infect. Dis.* **19,** 437–442
7. Padula, P. J., Edelstein, A., Miguel, S. D., Lopez, N. M., Rossi, C. M., and Rabinovich, R. D. (1998) *Virology* **241,** 323–330
8. Pensiero, M. N., Sharefkin, J. B., Dieffenbach, C. W., and Hay, J. (1992) *J. Virol.* **66,** 5929–5936
9. Zaki, S. R., Greer, P. W., Coffield, L. M., Goldsmith, C. S., Nolte, K. B., Foucar, K., Feddersen, R. M., Zumwalt, R. E., Miller, G. L., and Khan, A. S. (1995) *Am. J. Pathol.* **146,** 552–579
10. Nolte, K. B., Feddersen, R. M., Foucar, K., Zaki, S. R., Koster, F. T., Madar, D., Merlin, T. L., McFeeley, P. J., Umland, E. T., and Zumwalt, R. E. (1995) *Hum. Pathol.* **26,** 110–120
11. Gott, P., Zoller, L., Darai, G., and Bautz, E. K. (1997) *Virus Genes* **14,** 31–40
12. Lundkvist, A., Meisel, H., Koletzki, D., Lankinen, H., Cifire, F., Geldmacher, A., Sibold, C., Gott, P., Vaheri, A., Kruger, D. H., and Ulrich, R. (2002) *Viral Immunol.* **15,** 177–192
13. Maes, P., Keyaerts, E., Bonnet, V., Clement, J., Avsic-Zupanc, T., Robert, A., and Van Ranst, M. (2006) *Intervirology* **49,** 253–260
14. Geldmacher, A., Skrastina, D., Borisova, G., Petrovskis, I., Kruger, D. H., Pumpens, P., and Ulrich, R. (2005) *Vaccine* **23,** 3973–3983
15. Geldmacher, A., Skrastina, D., Petrovskis, I., Borisova, G., Berriman, J. A., Roseman, A. M., Crowther, R. A., Fischer, J., Musema, S., Gelderblom, H. R., Lundkvist, A., Renhofa, R., Ose, V., Kruger, D. H., Pumpens, P., and Ulrich, R. (2004) *Virology* **323,** 108–119
16. Kaukinen, P., Vaheri, A., and Plyusnin, A. (2005) *Arch. Virol.* **150,** 1693–1713
17. Maeda, A., Lee, B. H., Yoshimatsu, K., Saijo, M., Kurane, I., Arikawa, J., and Morikawa, S. (2003) *Virology* **305,** 288–297
18. Lee, B. H., Yoshimatsu, K., Maeda, A., Ochiai, K., Morimatsu, M., Araki, K., Ogino, M., Morikawa, S., and Arikawa, J. (2003) *Virus Res.* **98,** 83–91
19. Kaukinen, P., Vaheri, A., and Plyusnin, A. (2003) *Virus Res.* **92,** 37–45
20. Li, X. D., Makela, T. P., Guo, D., Soliymani, R., Koistinen, V., Vapalahti, O.,

Vaheri, A., and Lankinen, H. (2002) *J. Gen. Virol.* **83,** 759–766
21. Ravkov, E. V., Nichol, S. T., Peters, C. J., and Compans, R. W. (1998) *J. Virol.* **72,** 2865–2870
22. Ramanathan, H. N., Chung, D. H., Plane, S. J., Sztul, E., Chu, Y. K., Guttieri, M. C., McDowell, M., Ali, G., and Jonsson, C. B. (2007) *J. Virol.* **81,** 8634–8647
23. Khaiboullina, S. F., Rizvanov, A. A., Deyde, V. M., and St Jeor, S. C. (2005) *J. Med. Virol.* **75,** 267–275
24. Gott, P., Stohwasser, R., Schnitzler, P., Darai, G., and Bautz, E. K. (1993) *Virology* **194,** 332–337
25. Severson, W., Partin, L., Schmaljohn, C. S., and Jonsson, C. B. (1999) *J. Biol. Chem.* **274,** 33732–33739
26. Mir, M. A., and Panganiban, A. T. (2004) *J. Virol.* **78,** 8281–8288
27. Mir, M. A., and Panganiban, A. T. (2005) *J. Virol.* **79,** 1824–1835
28. Mir, M. A., Brown, B., Hjelle, B., Duran, W. A., and Panganiban, A. T. (2006) *J. Virol.* **80,** 11283–11292
29. Alfadhli, A., Love, Z., Arvidson, B., Seeds, J., Willey, J., and Barklis, E. (2001) *J. Virol.* **75,** 2019–2023
30. Kaukinen, P., Vaheri, A., and Plyusnin, A. (2003) *J. Virol.* **77,** 10910–10916
31. Yoshimatsu, K., Lee, B. H., Araki, K., Morimatsu, M., Ogino, M., Ebihara, H., and Arikawa, J. (2003) *J. Virol.* **77,** 943–952
32. Kaukinen, P., Kumar, V., Tulimaki, K., Engelhardt, P., Vaheri, A., and Plyusnin, A. (2004) *J. Virol.* **78,** 13669–13677
33. Alfadhli, A., Steel, E., Finlay, L., Bachinger, H. P., and Barklis, E. (2002) *J. Biol. Chem.* **277,** 27103–27108
34. Alminaite, A., Halttunen, V., Kumar, V., Vaheri, A., Holm, L., and Plyusnin, A. (2006) *J. Virol.* **80,** 9073–9081
35. Boudko, S. P., Kuhn, R. J., and Rossmann, M. G. (2007) *J. Mol. Biol.* **366,** 1538–1544
36. Delaglio, F., Grzesiek, S., Vuister, G. W., Zhu, G., Pfeifer, J., and Bax, A. (1995) *J. Biomol. NMR* **6,** 277–293
37. Johnson, B. A. (2004) *Methods Mol. Biol.* **278,** 313–352
38. Grzesiek, S., and Bax, A. (1993) *J. Am. Chem. Soc.* **115,** 12593–12594
39. Grzesiek, S., Dobeli, H., Gentz, R., Garotta, G., Labhardt, A. M., and Bax, A. (1992) *Biochemistry* **31,** 8180–8190
40. Wittekind, M., and Mueller, L. (1993) *J. Magn. Reson.* **101B,** 201–205
41. Muhandiram, D. R., and Kay, L. E. (1994) *J. Magn. Reson. Ser. B* **103** 203–216
42. Wishart, D. S., and Nip, A. M. (1998) *Biochem. Cell Biol.* **76,** 153–163
43. Tolman, J. R., Chung, J., and Prestegard, J. H. (1992) *J. Magn. Reson.* **98** 462–467
44. Grzesiek, S., and Bax, A. (1993) *J. Biomol. NMR* **3,** 185–204
45. Fesik, S. W., and Zuiderweg, E. R. P. (1998) *J. Magn. Reson.* **78** 588–593
46. Marion, D., Driscoll, P. C., Kay, L. E., Wingfield, P. T., Bax, A., Gronenborn, A. M., and Clore, G. M. (1989) *Biochemistry* **28,** 6150–6156
47. Guntert, P. (2004) *Methods Mol.Biol.* **278,** 353–378
48. Case, D. A., Pearlman, D. A., Caldwell, J. W., Cheatham Iii, T. E., Wang, J., Ross, W. S., Simmerling, C. L., Darden, T. A., Merz, K. M., Stanton, R. V., Cheng, A. L., Vincent, J. J., Crowley, M., Tsui, V., Gohlke, H., Radmer, R. J., Duan, Y., Pitera, J., Massova, I., Seibel, G. L., Singh, U. C., Weiner, P. K., and Kollman, P. A. (2002) *AMBER7*, University of California, San Francisco
49. Dames, S. A., Martinez-Yamout, M., De Guzman, R. N., Dyson, H. J., and Wright, P. E. (2002) *Proc. Natl. Acad. Sci. U. S. A.* **99,** 5271–5276
50. Laskowski, R. A., Rullmannn, J. A., MacArthur, M. W., Kaptein, R., and Thornton, J. M. (1996) *J. Biomol. NMR* **8,** 477–486
51. Baker, N. A., Sept, D., Joseph, S., Holst, M. J., and McCammon, J. A. (2001) *Proc. Natl. Acad. Sci. U. S. A.* **98,** 10037–10041
52. Deyde, V. M., Rizvanov, A. A., Chase, J., Otteson, E. W., and St Jeor, S. C. (2005) *Virology* **331,** 307–315
53. Choy, N., Raussens, V., and Narayanaswami, V. (2003) *J. Mol. Biol.* **334,** 527–539
54. Kiss, R. S., Kay, C. M., and Ryan, R. O. (1999) *Biochemistry* **38,** 4327–4334
55. Zhou, N. E., Zhu, B. Y., Kay, C. M., and Hodges, R. S. (1992) *Biopolymers* **32,** 419–426
56. Spiropoulou, C. F. (2001) *Curr. Top. Microbiol. Immunol.* **256,** 33–46